

Valence state of chromium ions in the half-metallic ferromagnet CrO₂ probed by ⁵³Cr NMRY. V. Piskunov ¹, A. F. Sadykov ¹, V. V. Ogloblichev ^{1,*}, A. G. Smolnikov ¹, A. P. Gerashenko,¹ and P. Z. Si ²¹*M. N. Mikheev Institute of Metal Physics of Ural Branch of Russian Academy of Sciences, Ekaterinburg 620108, Russia*²*Zhejiang Key Lab of Magnetic Materials, China Jiliang University, Hangzhou 310018, People's Republic of China*

(Received 28 April 2022; revised 14 July 2022; accepted 13 September 2022; published 23 September 2022)

We have performed ⁵³Cr NMR measurements on a high-purity polycrystalline sample to investigate the static and dynamic properties of a half-metallic ferromagnet CrO₂. Two ⁵³Cr NMR lines, corresponding to magnetically nonequivalent Cr nuclei, were observed in the ferromagnetic phase of CrO₂ despite all of the Cr ions being situated on the crystallographic equivalent sites. We measured the temperature dependences of the ⁵³Cr spin-lattice relaxation rate $(T_1)^{-1}$ in the ferromagnetic phase for the temperature range $T = 4.2\text{--}360$ K. It was found that in the range of low temperatures ($T \leq 60$ K) the relaxation of nuclear magnetic moments is determined mainly by the orbital contribution proportional to the temperature, conditioned by the fluctuation of the orbital currents of *d*-band electrons. At temperatures $T > 60$ K, the main mechanism leading to the nuclear spin-lattice relaxation is a three-magnon process of scattering at which the relaxation of the nuclear spin is accompanied by the absorption of a magnon and the creation of two magnons. Based on the analysis of temperature dependences of $(T_1)^{-1}$ for two nonequivalent Cr ions, we found that their valence state is the same and corresponds to valence Cr⁴⁺, whereas the difference of resonance frequencies for these ion nuclei is conditioned by the different magnetic local fields in their location.

DOI: [10.1103/PhysRevB.106.094428](https://doi.org/10.1103/PhysRevB.106.094428)

I. INTRODUCTION

Chromium dioxide CrO₂ belongs to a special class of highly spin-polarized half-metallic ferromagnets in which the density of states at the Fermi level, $N(E_F)$, is finite for the majority-spin state and close to zero for the minority-spin direction [1–4], producing conduction-band electron spin polarization (P) near 100% [5–7]. These properties make CrO₂ a very attractive candidate for future spintronic devices.

CrO₂ ($3d^2$), a ferromagnet with the Curie temperature $T_C = 395$ K, has a rutile structure (space group $P4_2/mnm = D_{4h}^{14}$) with $a = 4.421$ Å, $c = 2.916$ Å ($c/a = 0.65958$) [8]. The Cr atoms form a body-centered-tetragonal lattice, and they are surrounded by slightly distorted oxygen octahedra. The octahedra surrounding Cr at the body's center and corner positions differ by 90° rotation about the c axis. The CrO₂ crystal structure is shown in Fig. 1. Solid gray lines show the elementary crystal cell. Colored planes denote the equatorial planes. Dashed lines show the oxygen octahedra surrounding each of the Cr atoms, consisting of four O atoms in the equatorial plane and two apical atoms. Magnetic moments of chromium ions lie in the equatorial planes of CrO₆ octahedra and directed along the crystal c axis. x , y , and z are the local axes of CrO₆ octahedra; X , Y , and Z are the principal axes of the ⁵³Cr hyperfine coupling tensor; and Y is the quantization axis. Octahedral surrounding of chromium ions leads to the splitting of $3d$ orbitals into a t_{2g} triplet and an excited e_g doublet. The e_g states with only two valence $3d$ electrons are irrelevant, and only the t_{2g} orbitals are occupied. The tetragonal symmetry

distorts the octahedra, which lifts the degeneracy of the t_{2g} orbitals into a d_{xy} ground state and $d_{yz\pm zx}$ excited states [2,3]. A double exchange mechanism for two electrons per Cr site has been proposed in [9]. According to this, one t_{2g} electron occupies the narrow majority d_{xy} band, whereas broad $d_{yz\pm zx}$ bands are partially occupied, resulting in the localized character of the d_{xy} electron and the itinerant character of $d_{yz\pm zx}$. Furthermore, the strong contribution of oxygen p states at the Fermi surface explains why CrO₂ is a metal and not a Mott insulator [3]. It was also shown that CrO₂ belongs to the class of compounds with a negative charge-transfer gap leading to self-doping [3].

Band calculations [1] showed that the magnetic moment in CrO₂ correlates very accurately with the atomic value $\mu_0 = 2\mu_B$ for the Cr⁴⁺ ion. The same value of the magnetic moment aligned along the crystal c -axis was found in the neutron diffraction study in Ref. [10]. Based on ⁵³Cr NMR measurements, Shim *et al.* proposed that there are two Cr sites with different spontaneous moments in spite of one crystallographic Cr site [11]. They concluded that two Cr ions in different noninteger valence states appear in CrO₂, and they can be written as Cr^{4± x} ($x = 1/3$), where the macroscopic valence and magnetic moments remain unchanged as Cr⁴⁺ and $2\mu_B$ per formula unit, respectively.

Recently, their conclusion was confirmed by the investigation of the temperature-dependent valence and spin states of Cr ions in CrO₂ nanorod powder by x-ray magnetic circular dichroism (XMCD) and soft-x-ray absorption spectroscopy (XAS) methods [12]. In the opinion of the authors, they received direct experimental evidence for the Cr³⁺-Cr⁴⁺ mixed-valent states in bulk CrO₂ (Cr^{3.8+}), demonstrating that the half-metallic ferromagnetism in CrO₂ originates from the

*ogloblichev@imp.uran.ru

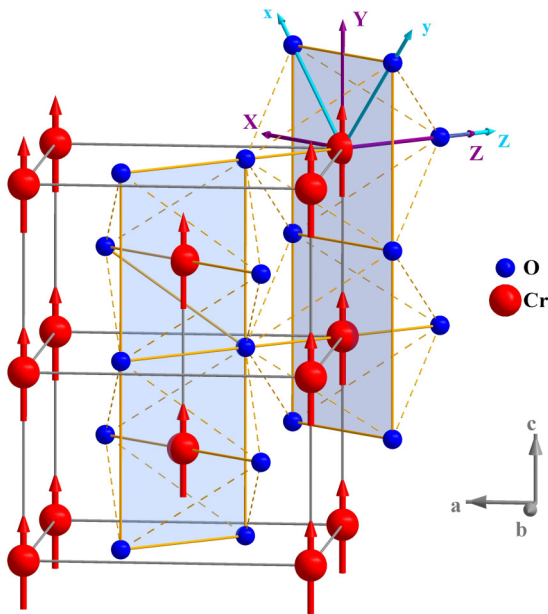


FIG. 1. CrO_2 crystal structure. Solid gray lines show the elementary crystal cell. Colored planes denote the equatorial planes. Dashed lines show the oxygen octahedra surrounding each Cr atom, consisting of four O atoms in the equatorial plane and two apical atoms. Magnetic moments of chromium ions lie in the equatorial planes of CrO_6 octahedra and directed along the crystal c axis. x , y , z are the local axes of CrO_6 octahedra; X , Y , Z are the principal axes of the ^{53}Cr hyperfine coupling tensor.

double-exchange interaction. On the other hand, the analysis of the hyperfine field performed in the NMR investigation [13] showed the presence of two Cr sites with different orbital occupancies, suggesting that a local orbital order takes place upon breaking the local symmetry in the rutile structure. This may be ascribed to the negative charge transfer between chromium and oxygen ions. Takeda *et al.* found that the two Cr sites do not have different valence states, but the $3d$ orbital occupation numbers are different from each other.

In this study, we performed ^{53}Cr NMR measurements on a polycrystalline sample of CrO_2 in the ferromagnetic phase, and we observed two sets of ^{53}Cr spectra corresponding to chromium at the crystallographic equivalent sites Cr(A) and Cr(B). The analysis of the temperature dependences of the spin-lattice relaxation rates of chromium nuclear moments in the temperature range $T = 4.2\text{--}360$ K showed that the chromium ions in the Cr(A) and Cr(B) sites have the same valence state Cr^{4+} .

II. EXPERIMENTAL DETAILS

The high-purity CrO_2 sample used in this study was prepared by decomposing CrO_3 in O_2 with gas pressures up to 40 MPa, which were maintained throughout the decomposition process of CrO_3 to prevent the formation of any other phases of chromium oxides. The process of synthesis, and the structural and magnetic properties of the investigated sample CrO_2 , were described in detail in Ref. [14]. The lattice parameters of CrO_2 were $a = 4.4176$ Å and $c = 2.9144$ Å. The SEM data showed that the samples were rod-shaped particles with a length of 3–7 μm. X-ray diffraction measurements

have shown no diffraction peaks of the other chromium oxides in the compound [14].

The ^{53}Cr ($I = 3/2$) NMR measurements were performed with the Bruker pulse spectrometer AVANCE III at zero external magnetic field within the temperature range from 4.2 to 365 K. The NMR ^{53}Cr spectra were obtained by the standard spin-echo pulse sequence $\tau_p\text{--}t_{\text{del}}\text{--}\tau_p\text{--}t_{\text{del}}\text{--}echo$ with $\tau_p \leq 1.5$ μs and $t_{\text{del}} = 50$ μs. The temperature-dependent measurements were carried out using a flow cryostat (Oxford Instruments, UK) with a constant cooling gas flow (N_2 or He for temperatures $T < 80$ K). In all the experiments, the measurement and stabilization of the sample temperature ($\Delta T/T \leq 0.05$) were performed by the temperature controller ITC 5 (Oxford Instruments, UK). When recording broad spectra, the width of which exceeds the frequency band excited by the rf pulse, the summation procedure was applied to the array of signals accumulated within the required frequency range with steps of $\Delta\nu = 150$ kHz. Measurements of the spin-lattice relaxation time T_1 were performed by the inversion recovery method using the pulse sequence $2\tau_p\text{--}t_{\text{inv}}\text{--}\tau_p\text{--}t_{\text{del}}\text{--}\tau_p\text{--}t_{\text{del}}\text{--}echo$ with $t_{\text{del}} = 50$ μs in the interval t_{inv} from $0.01T_1$ to $10T_1$ [15,16].

III. RESULTS AND DISCUSSION

Figure 2(a) shows ^{53}Cr NMR spectra of polycrystalline CrO_2 at temperatures $T = 4.2$ and 293 K in zero magnetic field. ^{53}Cr NMR spectra consist of two narrow lines Cr(A) and Cr(B) at 26.3 and 37.1 MHz ($T = 4.2$ K) with a full width at half-maximum (FWHM) of 0.20 and 0.30 MHz, respectively. The positions of the line peaks coincide with the previous NMR results [11,13,17], but the FWHM is two to three times less. This speaks to the very good quality of our CrO_2 samples. The integral intensities of ^{53}Cr NMR lines on Cr(A) and Cr(B) sites at $T = 4.2$ K are approximately equal; the difference between the peaks of lines is 10.76 MHz. Both ^{53}Cr NMR lines are slightly asymmetrical. The Cr(A) line has the asymmetry to the side of higher frequencies, while the Cr(B) line has the asymmetry to the lower frequencies. At the increase of temperature up to room temperature, both ^{53}Cr NMR lines become narrower and move to the side of fewer frequencies due to the decrease of sample magnetization $M(T)$. The difference between them decreases to 10.48 MHz. The relative intensities of the lines almost do not change, though the Cr(B) line narrows with the increase of temperature more than the line Cr(A). As a result, the relationship of the Cr(A) and Cr(B) line amplitudes at the temperature transition from $T = 4.2$ to 293 K reverses. The NMR linewidth is determined by two factors: dynamic and static. The dynamic factor determines the so-called uniform linewidth. It is related to the lifetime of the nuclear spin at a particular energy level. In this case, the linewidth is proportional to the spin-spin and spin-lattice relaxation rates $1/T_2$ and $1/T_1$. This broadening factor is typical for liquids and gases. As for solids, the main factor in NMR line broadening is practically always the static factor due to static inhomogeneities of the internal magnetic field (inhomogeneous broadening). In solid CrO_2 , we deal exclusively with inhomogeneous line broadening. The distribution of magnetic moments of Cr ions in the sample is inhomogeneous, which leads to broadening. As the temperature

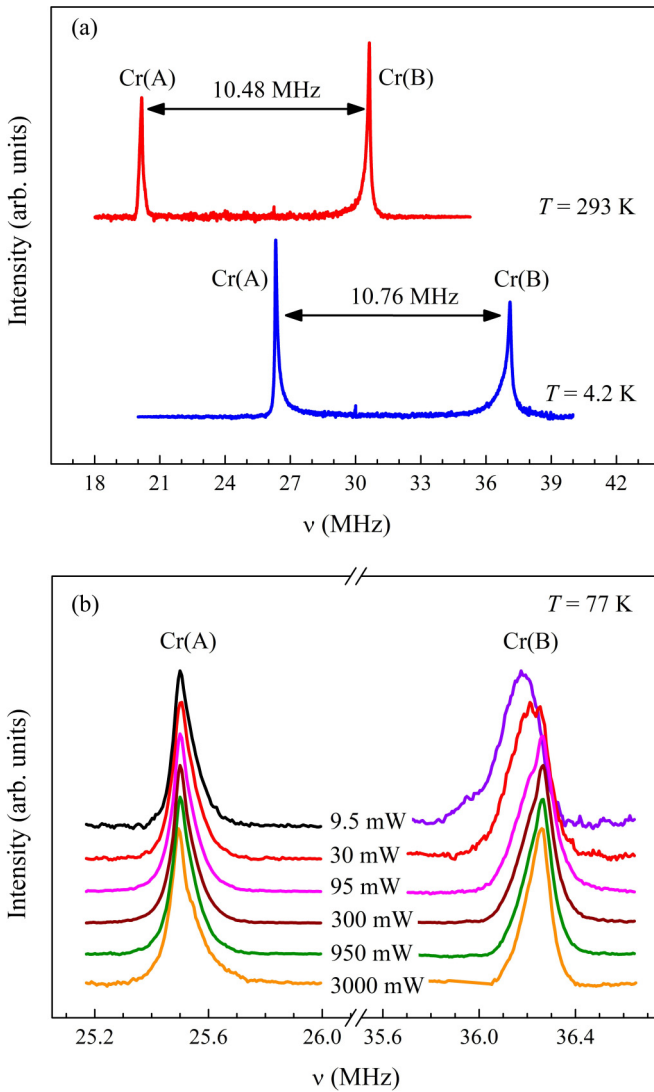


FIG. 2. (a) ^{53}Cr NMR spectra at temperatures $T = 4.2$ and 293 K. Two lines in the NMR ^{53}Cr spectrum correspond to the chromium nuclei in positions Cr(A) and Cr(B). (b) ^{53}Cr NMR spectra, measured at the different power of spectrometer radiofrequency transmitter.

increases, the static inhomogeneities of the field inside the sample are averaged due to motion. Therefore, as the temperature increases, the NMR ^{53}Cr lines become narrower.

The narrowness of the NMR Cr(A) and Cr(B) lines in the CrO_2 powder is due to the fact that in the zero external magnetic field, in all the microcrystals the local magnetic field, produced by the magnetic moments of Cr ions, is directed in the same way with respect to the crystal lattice axes (namely along the c axis). This direction of the local magnetic field is a quantization axis of nuclear magnetic moments. The application of an external magnetic field of magnitude $H \geq 0.4$ T leads to the rotation of the magnetic moments of chromium ions in all microcrystallites along the direction of the external magnetic field [13]. In the case of the powder, the direction of the internal local field will be distributed inside the solid angle 360° relative to crystal lattice axes. This will lead to a multiple broadening of the NMR spectrum. In other words,

in this case we will move from the “single-crystal mode” to the “polycrystal mode.” In this work, we studied nuclear spin-lattice relaxation. We needed to make the NMR lines as narrow as possible. Therefore, we carried out all experiments in a zero external magnetic field.

In previous works [11,13,17], it was definitely proved that both Cr(A) and Cr(B) lines correspond to the chromium that is located inside the magnetic domains and not in the domain walls. As for the signal from Cr in the domain walls, it is not observed, probably due to the small relative volume of these walls in crystallites and/or the short time of nuclear spin-spin relaxation T_2 . We have evaluated the enhancement factor as $\eta = 30$ in our measurements of NMR ^{53}Cr spectra in the following way. As we know, the intensity of the radiofrequency field H_1 necessary to rotate the nuclear magnetization by 90° is expressed as $H_1 = \frac{\pi}{2\gamma_n\tau_p}$, where γ_n is the nuclear gyromagnetic ratio and τ_p is the duration of the 90° pulse [15]. On the other hand, the transmitter power P required to generate the field H_1 in the coil with the sample is determined by the following expression: $P \approx \frac{\nu_0 V}{9Q} H_1^2$, where ν_0 is the resonance frequency, V is the internal volume of the coil, and Q is the circuit quality factor [15]. Combining the above two expressions, we obtain an expression for the transmitter power at the 90° pulse: $P \approx \frac{\pi^2 \nu_0 V}{36Q\gamma_n^2 \tau_p^2}$. In the presence of amplification effects, power $P^* = P/\eta^2$ is sufficient for the 90° rotation of nuclear magnetization. Thus, we may determine $\eta = \sqrt{P/P^*}$ by measuring the transmitter power at the 90° pulse with (P^*) and without (P) amplification effects at constant values ν_0 , V , Q , γ_n , and τ_p . We used ^{25}Mg NMR in MgB_2 at the external field $H_0 = 9.28$ T to determine the power P . These resonance nuclei have been chosen because the resonant frequency $^{25}\nu_0 = 24.3$ MHz in the field $H_0 = 9.28$ T is close to the resonant frequency of ^{53}Cr [Cr(A) site at $T = 77$ K] $^{53}\nu_0 = 25.5$ MHz in the local field [Fig. 2(b)]. Besides, the value $^{25}\gamma_n/2\pi = 0.260$ MHz/kOe is very close to $^{53}\gamma_n/2\pi = 0.240$ MHz/kOe. As a result, we have obtained that $P = 300$ W, $P^* = 0.3$ W, and $\eta = \sqrt{\frac{P}{P^*}} \approx 30$. This value of $\eta = 30$ is a typical enhancement factor for domains of ferromagnets, and it is too small compared with $\eta = 10^3$ – 10^4 in domain walls [18].

Figure 2(b) shows the normalized NMR Cr(A) and Cr(B) lines, recorded with the fixed impulse time τ_p , but at different power levels of a radiofrequency transmitter. As can be seen from Fig. 2(b), the position and shape of the NMR Cr(A) line almost do not change depending on the power of the transmitter (only the intensity changed; the signal at 9.5 mW in 10 times smaller than at 300 mW). As for the NMR Cr(B) line, it changes shape and shifts to lower frequencies with decreasing pulse power. As we mentioned above, the Cr(B) line has the asymmetry to the side of lower frequencies. Apparently, the chromium nuclei corresponding to this low-frequency part of the spectrum Cr(B) have a larger enhancement factor than the main signal of position Cr(B). In this case, a low transmitter power (9.5 mW) leads to stronger suppression of the main line compared to the low-frequency part of the spectrum Cr(B). Conversely, high transmitter power suppresses the low-frequency pedestal of the Cr(B) line. All this leads to the picture that is observed in Fig. 2(b). Namely, as the transmitter power decreases, the NMR Cr(B) line will broaden and shift

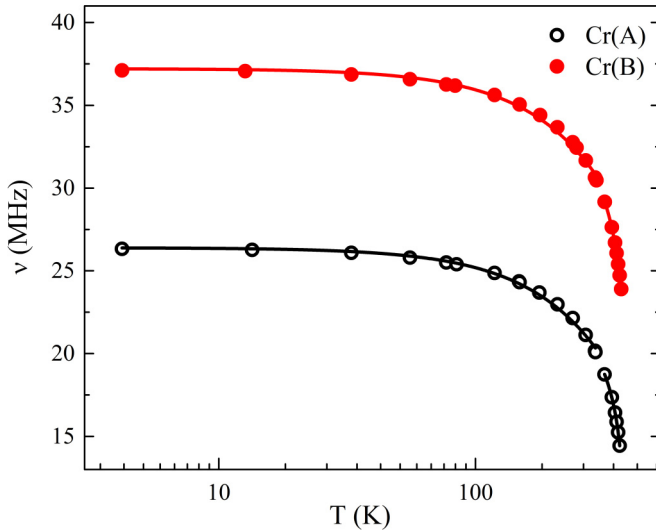


FIG. 3. The dependencies of resonance frequencies of chromium nuclei in positions Cr(A) and Cr(B) on the temperature. Solid lines show the result of data approximation by functions $\nu_n(T) = \nu_n(T=0)(1 - aT^{3/2})$ (at $T \leq 300$ K) and $\nu_n(T) = \nu_n(T=0)k(T_C - T)^\beta$ (at $T \geq 300$ K). The measurement error did not exceed the symbol size.

to the low-frequency region. This effect is less noticeable in the Cr(A) line, since its asymmetry is less pronounced than in the Cr(B) line. We cannot unambiguously determine the nature of the asymmetry of the Cr(A) and Cr(B) lines. It might be associated with the presence of a small signal from the domain walls. However, taking into account estimates of the anisotropy of local magnetic fields $H_{n,\alpha}$ by Takeda *et al.* [13], this may be the case only if the magnetic moments in the domain wall rotate in the plane xy of CrO_6 octahedra. Such an asymmetry may also be due to of the lattice distortions and the surface effects.

In the general case for ^{53}Cr with spin $I = 3/2$ and the electrical quadrupole moment $e^{53}Q = 0.150 \times 10^{-24} \text{ cm}^2$, one should observe $2I = 3$ lines: one corresponding to the central transition ($m_1 = -1/2 \leftrightarrow 1/2$) and two so-called satellite lines ($m_1 = -3/2 \leftrightarrow -1/2$, $1/2 \leftrightarrow 3/2$). However, distinctly separated lines as, e.g., in [19,20] are not observed in ^{53}Cr NMR spectra in CrO_2 . It is possible that the quadrupole splitting is hidden in the spectrum width [21].

Resonance frequencies of Cr(A) and Cr(B) lines are determined by the inner magnetic field \mathbf{H}_n , which is the sum of the hyperfine field \mathbf{H}_{hf} , the classical dipole field \mathbf{H}_D , the demagnetization field \mathbf{H}_{dem} , and the Lorentz field \mathbf{H}_L . Each of them is proportional to the magnetic moment of the chromium ion [18]: $\mathbf{H}_n = \mathbf{H}_{\text{hf}} + \mathbf{H}_D + \mathbf{H}_{\text{dem}} + \mathbf{H}_L = A_n \mathbf{M}$. Therefore, the temperature dependence of the NMR Cr(A) and Cr(B) line frequency is completely defined by the T -dependence of the magnetic moment of the chromium ion.

Figure 3 shows the dependencies of resonance frequencies of chromium ions in positions Cr(A) and Cr(B) versus T . In the temperature range $T \leq 300$ K, the data are in good agreement with the Bloch law [22]:

$$\frac{\nu_n(T)}{\nu_n(T=0)} = [1 - aT^{3/2}], \quad (1)$$

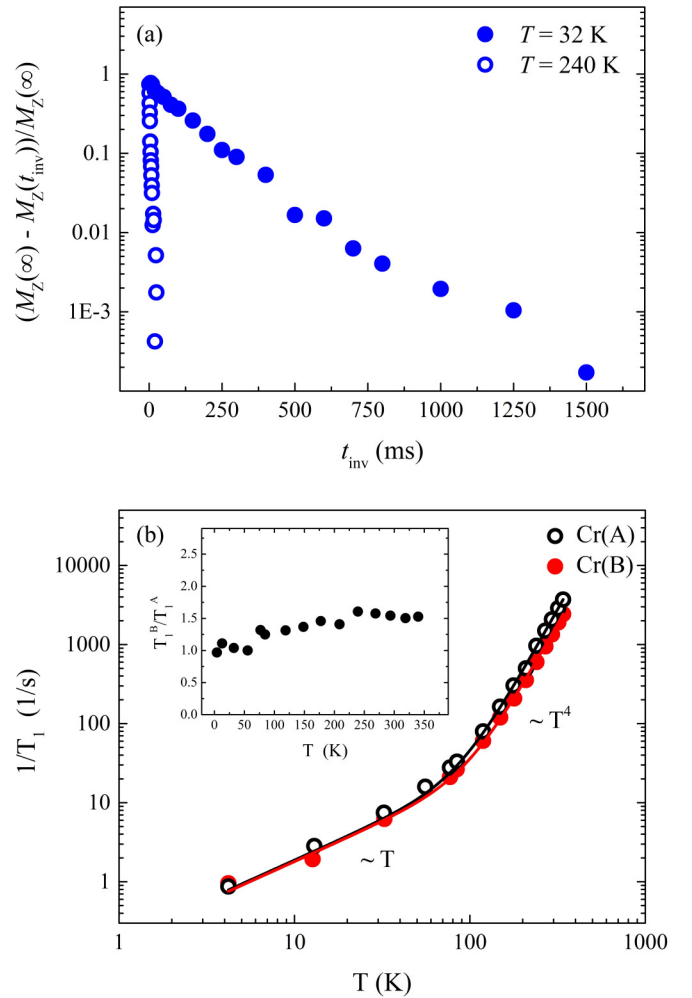


FIG. 4. (a) Recovery of ^{53}Cr nuclear magnetizations $^{53}M_Z(t)$ shown in a semilog scale of the quantity $^{53}m(t) = [M_Z(\infty) - M_Z(t)]/M_Z(\infty)$ vs the time interval t_{inv} after applying an inversion rf pulse at $T = 240$ K (open circles) and $T = 32$ K (closed circles). (b) Temperature dependencies of spin-lattice relaxation rates of chromium nuclei in positions Cr(A) and Cr(B). The data were approximated by a function $1/T_1 = AT + BT^n$. Inset: temperature dependence of the relationship of times of relaxation. The measurement error did not exceed the symbol size.

but they deviate significantly from it in the range of higher temperatures. At $T \geq 300$ K, the dependencies were approximated by the expression $\frac{\nu_n(T)}{\nu_n(T=0)} = k(T_C - T)^\beta$, which describes the critical behavior of magnetization near the Curie temperature T_C . Here k is the proportionality factor, and β is the critical index. The best agreement with the experimental data has been obtained at the following approximation parameters: $k = 0.34$, $T_C = 390$ K, $\beta = 0.18$.

We measured the spin-lattice relaxation rate T_1^{-1} for Cr(A) and Cr(B) as a function of temperature. The recovery of ^{53}Cr nuclear magnetizations $^{53}M_Z(t)$ shown in a semilog scale of the quantity $^{53}m(t) = [M_Z(\infty) - M_Z(t)]/M_Z(\infty)$ versus the time interval t_{inv} after applying an inversion rf pulse at $T = 240$ K (open circles) and $T = 32$ K (closed circles) is displayed in Fig. 4(a). The results are summarized in Fig. 4(b), plotted as $(T_1)^{-1}$ versus temperature. In the low-temperature

range $T < T_C/6$, $(T_1)^{-1}(T)$ demonstrates a Korringa-like linear temperature dependence T . At higher temperatures, $T > T_C/4$, the relaxation rate increases more rapidly than the linear T relation, suggesting that the relaxation mechanisms, involving spin-wave excitations (magnons), become important in this range.

In the general case, the nuclear spin-lattice relaxation in ferromagnetic transition metals is determined by several contributions:

$$\left(\frac{1}{T_1}\right)_{\text{meas}} = \left(\frac{1}{T_1}\right)_s + \left(\frac{1}{T_1}\right)_{\text{cp}} + \left(\frac{1}{T_1}\right)_{\text{dip}} + \left(\frac{1}{T_1}\right)_{\text{orb}} + \left(\frac{1}{T_1}\right)_Q + \left(\frac{1}{T_1}\right)_m. \quad (2)$$

Let us consider each term in (2) separately:

$$\left(\frac{1}{T_1}\right)_s = \pi \hbar k_B \gamma_n^2 \left(\frac{16\pi \mu_B}{3}\right)^2 T \langle |\psi_s(0)|^2 \rangle_{F\uparrow} \langle |\psi_s(0)|^2 \rangle_{F\downarrow} \times N_{s\uparrow}(E_F) N_{s\downarrow}(E_F) \quad (3)$$

is the contact or Korringa contribution [23,24]. Here k_B is the Boltzmann constant, γ_n is the gyromagnetic ratio of the nucleus, μ_B is the Bohr magneton, $\langle \rangle_{F\uparrow(\downarrow)}$ is the average over the Fermi surface for the up (down) spin s electrons, and $N_{s\uparrow(\downarrow)}(E_F)$ is the density of states per atom for the up (down) spin s electrons at the Fermi energy. The next term,

$$\left(\frac{1}{T_1}\right)_{\text{cp}} = 4\pi \gamma_n^2 k_B T N_{d\uparrow}(E_F) N_{d\downarrow}(E_F) q A_{\text{cp}}^2, \quad (4)$$

comes from relaxation induced by core polarization, where A_{cp} is the hyperfine core polarization coupling constant, and q is the coefficient depending on the degeneration degree of the orbital d -states [25,26]. The third term in (2) represents the relaxation due to the dipolar interaction of nuclei with the conduction electrons, and it can be expressed in the following way [27]:

$$\left(\frac{1}{T_1}\right)_{\text{dip}} = \pi \hbar k_B \gamma_n^2 \mu_B^2 T \langle 1/r^3 \rangle_F^2 N_{d\uparrow}(E_F) N_{d\downarrow}(E_F) F(C). \quad (5)$$

Here $\langle 1/r^3 \rangle_F$ is the average of the d -electron radii over the Fermi surface, and $F(C)$ is a function of C parameter. This parameter is defined as follows: $3C + 2D = 5$. C and D represent the degree of admixture of t_{2g} atomic functions (belonging to the cubic group Γ_5) and e_g (cubic group Γ_3), respectively, in the Bloch wave functions at the Fermi surface.

As was mentioned above, CrO_2 is a half-metal with almost 100% degree of polarization of conduction electrons [5–7]. In the given substance, there is a gap in the density of state at the Fermi energy for the down-spin electrons, so $N_{s\downarrow}(E_F) = 0$. In the above three relaxation processes, the electron spin flips to flip the nuclear spin. However, the flip is not allowed from the 100% electron spin polarization. Hence it appears that all three of the above contributions $(\frac{1}{T_1})_s$, $(\frac{1}{T_1})_{\text{cp}}$, and $(\frac{1}{T_1})_{\text{dip}}$ in CrO_2 are equal to zero.

The fourth term in (2) is the so-called orbital contribution, conditioned by the fluctuation of the orbital currents of d -band electrons. In the orbital relaxation processes, the electrons are scattered by nuclear spins without changing their own spins.

Therefore, the electrons with up and down spins make independent additive contributions to the nuclear spin relaxation rate [24,27]:

$$\left(\frac{1}{T_1}\right)_{\text{orb}} = \pi \hbar k_B \gamma_n^2 \mu_B^2 T \langle 1/r^3 \rangle_F^2 \{ [N_{d\uparrow}(E_F)]^2 + [N_{d\downarrow}(E_F)]^2 \} \times (16/5)[1 - (C - 1)^2], \quad (6)$$

where C is the same parameter that occurs in the expression (5). It can have values from 0 to 5/3. Since in CrO_2 the wave functions at the Fermi surface have only $t_{2g}(\Gamma_5)$ character [$e_g(\Gamma_3)$ states are above Fermi energy [3]], $D = 0$ and $C = 5/3$. And then, in the CrO_2 case, the expression (6) will look like this:

$$\left(\frac{1}{T_1}\right)_{\text{orb}} = (16/9)\pi \hbar k_B \gamma_n^2 \mu_B^2 T \langle 1/r^3 \rangle_F^2 [N_{d\uparrow}(E_F)]^2. \quad (7)$$

Since in the transition metals the density of states of $3d$ electrons at the Fermi surface is usually rather large, the orbital contribution to them can also be rather significant.

The quadrupole contribution $(\frac{1}{T_1})_Q$ to the relaxation is conditioned by the interaction of nuclear spins with the fluctuations of electric field gradient induced by the electric charges that surround the nucleus. It can be presented in the form of two terms that describe lattice vibrations (phonon contribution) and conduction electrons (electron contribution). The first one is effective in the ion crystals and can be neglected in metals. The second contribution is proportional to the squares of the quadrupole moment of nuclear Q , the electric field gradient eQ , and the density of states [28]:

$$\left(\frac{1}{T_1}\right)_Q \propto (e^2 q Q)^2 k_B T \{ [N_{d\uparrow}(E_F)]^2 + [N_{d\downarrow}(E_F)]^2 \}. \quad (8)$$

In the transition metals, this contribution is two orders of magnitude less than the orbital [24,28], which is why it can be neglected.

The last term in (2) describes the processes of spin-lattice relaxation, conditioned by inelastic scattering of spin waves (magnons) on nuclei, conducted by a nuclear spin flip. The theory of these processes in magnetic materials is described in detail in the work of Beeman and Pincus [29]. In this work, we consider briefly the magnon relaxation mechanisms with respect to the chromium dioxide.

The direct process in which a single magnon is created or absorbed while the nuclear spin is flipped is not allowed because of energy conservation; the change of energy due to the nuclear spin flip is much smaller than the minimum energy of the ferromagnetic spin wave $g\mu_B H_A$. Particularly in our experiments, where the crystalline anisotropy field is $H_A \approx 4$ kOe [13], the minimum magnon frequency $\nu_{\text{min}} = \omega_{\text{min}}/2\pi = 11.2$ GHz is three orders of magnitude larger than the NMR frequency. Therefore, the first process to be considered is the Raman relaxation process.

The essence of the two-magnon Raman mechanism is that in the relaxation process, the nuclear spin flip is conducted by the annihilation of a magnon with energy $\hbar\omega_k$ and the creation of a magnon with energy $\hbar\omega_{k'}$. At that, the equality $\hbar\omega_{k'} - \hbar\omega_k = \hbar\omega_{\text{NMR}}$, which ensures that the energy conservation is fulfilled. References [29–31] showed that the Raman process can make a contribution to the nuclear relaxation

only in two cases: if the tensor of the hyperfine interaction in the X , Y , and Z coordinate axes is anisotropic and contains nonzero nondiagonal members, and if the quantization axes of nuclear and electron spins do not coincide. In this case, $1/T_1 \propto (\sin^2\theta)T^2 \ln(T)$ [28], where θ is the angle between the quantization axes of nuclear and electron spins. In the case of CrO_2 , the spin-dipole hyperfine interaction of nuclear chromium spins with d -electrons makes the tensor of the full hyperfine interaction anisotropic. However, the orientation of d -orbitals of chromium ions in CrO_2 is such that the nondiagonal members of this tensor are equal to zero in the X , Y , and Z coordinate axes [3,4,32]. As for the mismatch of quantization axes of electron and nuclear spins, it can occur in the presence of quadrupole interaction when the main axis of the electric field gradient tensor does not coincide with the direction of the magnetic hyperfine field. In the case when the quadrupole interaction is much less than the hyperfine one, i.e., when the resonance frequency of the observed line is determined mainly by the local magnetic field, $\nu_{\text{res}} = \gamma_n h_{\text{loc}}$, $\sin\theta \sim \frac{\nu_Q}{\nu_{\text{res}}}$, where the quadrupole frequency $\nu_Q \propto e^2 q Q$ describes the value of the quadrupole interaction and determines the distance between satellite resonance lines in the quadrupole split NMR spectrum. Since the separate satellite lines in the NMR spectra are not observed (which means that they are inside the main observed lines), ν_Q can be evaluated as not exceeding 0.5 MHz. Therefore, the contribution of the two-magnon process to the spin-lattice relaxation of chromium nuclei in CrO_2 will be absent.

The above-mentioned restrictions do not occur at the three-magnon relaxation process. In this process, the relaxation of the nuclear spin is accompanied by the absorption of a magnon and the creation of two magnons. The only limitation for such a mechanism is the condition $2\omega_{\text{min}} \leq \omega_{\text{max}}$, where ω_{min} and ω_{max} are the minimum and the maximum frequencies correspondingly in the magnon excitation spectrum. The rate of nuclear relaxation in a ferromagnet, conditioned by the three-magnon processes, is determined by the following expression [29,33]:

$$\left(\frac{1}{T_1}\right)_{3m,\alpha} = \frac{7.6}{16(2\pi)^5} \frac{A_\beta^2 + A_\gamma^2}{\hbar^2 \omega_e S} \left(\frac{k_B T}{\hbar \omega_e}\right)^{7/2}, \quad (\alpha, \beta, \gamma = X, Y, Z). \quad (9)$$

Here A_α is the constant of magnetic hyperfine interaction, and S is the full spin of the magnetic ion. Taking into account that in ferromagnets $\hbar \omega_e = 2JS = 2(J_1 + J_2)S$, where J_1 and J_2 are the nearest-neighbor and next-nearest-neighbor exchange constants, respectively, the expression (9) can be written in the following way:

$$\left(\frac{1}{T_1}\right)_{3m,\alpha} = \frac{7.6}{16(2\pi)^5} \frac{A_\beta^2 + A_\gamma^2}{2J\hbar S^{11/2}} \left(\frac{k_B T}{2J}\right)^{7/2}. \quad (10)$$

Summing up, we can conclude that the nuclear spin-lattice relaxation of nuclei ^{53}Cr in CrO_2 is determined mainly by two terms:

$$\left(\frac{1}{T_1}\right)_{\text{meas}} = \left(\frac{1}{T_1}\right)_{\text{orb}} + \left(\frac{1}{T_1}\right)_{3m}, \quad (11)$$

the first of which is proportional to T , and the second to $T^{3.5}$. Since the quantization axis of nuclear spins in CrO_2

crystallites is directed along the Y axis (c axis of a crystal lattice), in the expression (10) $\alpha = Y$, $\beta = X$, $\gamma = Z$.

In Fig. 4(b) the temperature dependences of the nuclear spin-lattice relaxation rates, measured on the ions Cr(A) and Cr(B), were approximated by the expression $(T_1)^{-1} = AT + BT^n$, where A , B , and n were variable parameters. The best correspondence between the experimental data and the approximating lines has been achieved at the coefficients for Cr(A): $A = 0.19$, $B = 2.69 \times 10^{-7}$, $n = 4.0(2)$, and for Cr(B): $A = 0.18$, $B = 1.92 \times 10^{-7}$, $n = 3.9(2)$. As can be seen, the n is close enough to the theoretical value $n = 3.5$. As a result of this approximation, we have obtained that the relationship of coefficients B at T^4 for Cr(A) and Cr(B) is 1.4. Using Eq. (10), we obtain

$$\frac{B(\text{Cr(A)})}{B(\text{Cr(B)})} \equiv R = \frac{A_X^2(\text{Cr(A)}) + A_Z^2(\text{Cr(A)})}{A_X^2(\text{Cr(B)}) + A_Z^2(\text{Cr(B)})} \left[\frac{S(\text{Cr(B)})}{S(\text{Cr(A)})} \right]^{11/2} = 1.4(1), \quad (12)$$

or, proceeding from the constants of hyperfine interaction A_α to the local fields on the nuclear $H_{n,\alpha} = 2A_\alpha S$, we obtain

$$R = \frac{H_{n,X}^2(\text{Cr(A)}) + H_{n,Z}^2(\text{Cr(A)})}{H_{n,X}^2(\text{Cr(B)}) + H_{n,Z}^2(\text{Cr(B)})} \left[\frac{S(\text{Cr(B)})}{S(\text{Cr(A)})} \right]^{15/2} = 1.4(1). \quad (13)$$

In the inset of Fig. 4(b), the temperature dependence of the relationship of relaxation times $\frac{T_1^B}{T_1^A} = \frac{A(\text{Cr(A)})T + B(\text{Cr(A)})T^4}{A(\text{Cr(B)})T + B(\text{Cr(B)})T^{3.9}}$ is shown. Since at the low temperature ($T < 50$ K) $AT \gg BT^4$ and at high temperature ($T > 200$ K) $AT \ll BT^4$, we have $\frac{T_1^B}{T_1^A}(T < 50 \text{ K}) \cong \frac{A(\text{Cr(A)})}{A(\text{Cr(B)})}$ and $\frac{T_1^B}{T_1^A}(T > 200 \text{ K}) \cong \frac{B(\text{Cr(A)})}{B(\text{Cr(B)})}$. As is seen in the inset of Fig. 4(b), indeed $\frac{T_1^B}{T_1^A}(T < 50 \text{ K}) \cong \frac{A(\text{Cr(A)})}{A(\text{Cr(B)})} \cong 1$ and $\frac{T_1^B}{T_1^A}(T > 200 \text{ K}) \cong \frac{B(\text{Cr(A)})}{B(\text{Cr(B)})} \cong 1.4$ correspond to the results of the approximation in Fig. 4(b). The equality $A(\text{Cr(A)}) \cong A(\text{Cr(B)})$ means the equality of the density of states at the Fermi level $N_{d\uparrow}(E_F)$ for Cr(A) and Cr(B) sites [see Eq. (7)]. As mentioned above, the limitation for the three-magnon mechanism is the condition $2\omega_{\text{min}} \leq \omega_{\text{max}}$, where ω_{min} and ω_{max} are the minimum and the maximum frequencies correspondingly in the magnon excitation spectrum. Then, we can estimate the minimal width of the magnon band as $\Delta\nu_{\text{min}} = \omega_{\text{min}}/2\pi = g\mu_B H_A/h = 11.2$ GHz. Moreover, we have evaluated the interatomic exchange interaction $J = 730$ K by using Eq. (10), the data of Takeda *et al.* [13] for the hyperfine coupling constants [$A_X(\text{Cr(A)}) = 56$ kOe/ μ_B , $A_Z(\text{Cr(A)}) = 122$ kOe/ μ_B], and our result $1/T_1(\text{Cr(A)})$, $T = 300$ K) = 4×10^3 s $^{-1}$. It is almost two times larger than the estimate $J = 400$ K obtained theoretically in Ref. [34].

As was already mentioned in the Introduction, in Refs. [11] and [13] there appeared a disagreement on the questions of valence states of ions Cr(A) and Cr(B). In the earlier work [11] analyzing their NMR data, the authors concluded that the chromium ions in Cr(A) have valence $\text{Cr}^{4.34+}$, and ions Cr(B) respectively, $\text{Cr}^{3.66+}$. Their conclusion is based on the supposition that $H_{n,Y}(\text{Cr(A)}) \cong H_{n,Y}(\text{Cr(B)})$. In the second work of [13], based on a more thorough analysis of the local magnetic field $H_{n,\alpha}$, it was discovered that both the values of $H_{n,\alpha}$ and their anisotropy have an essential difference for

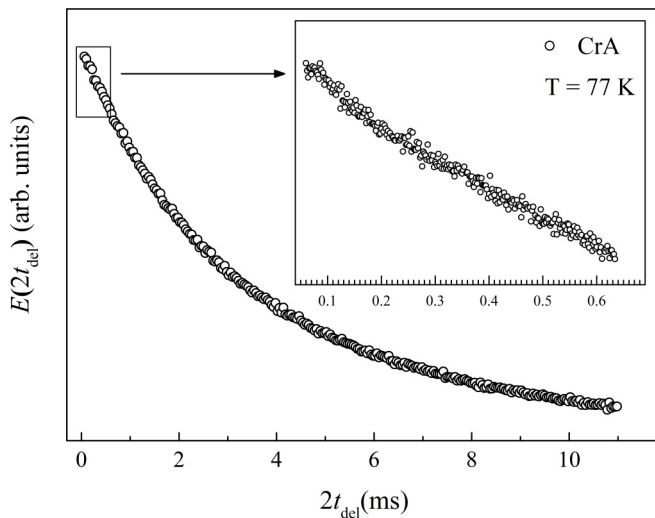


FIG. 5. The dependences of the spin echo decay $E(2t_{\text{del}})$ of ^{53}Cr [Cr(A) site] vs double delay between the pulses $2t_{\text{del}}$ in the CrO_2 at $T = 77$ K. Inset: the initial part $E(2t_{\text{del}})$, measured with the step $\Delta t_{\text{del}} = 1 \mu\text{s}$. The data for chromium in the Cr(B) position are not shown because of their identity with the data for chromium in the Cr(A) position.

chromium in the positions Cr(A) and Cr(B). From the data analysis, it was stated that $H_{n,\gamma}(\text{Cr(A)}) \neq H_{n,\gamma}(\text{Cr(B)})$, and $S(\text{Cr(A)}) \cong S(\text{Cr(B)})$, i.e., the valence state of ions Cr(A) and Cr(B) is almost identical, and their valence is practically equal to Cr^{4+} . If we use the values of $H_{n,\alpha}$, obtained in Ref. [13], then from the expression (13) we obtain that $\frac{S(\text{Cr(B)})}{S(\text{Cr(A)})} = 1.009(5)$.

Therefore, our data on the temperature dependencies of the nuclear spin-lattice relaxation in positions Cr(A) and Cr(B) also prove that the valence state of chromium ions in these positions is the same and corresponds to valence Cr^{4+} , and the difference of resonance frequencies for Cr(A) and Cr(B) nuclei is conditioned by the different magnetic local fields in the place of their location.

However, it is still not clear why in the crystallographically equivalent positions Cr(A) and Cr(B) chromium ions have a different distribution of charges over $3d$ orbitals. It is possible that CrO_6 octahedra with Cr(A) and Cr(B) ions in their centers are not completely equivalent and differ in size. In this case, one can expect the different quadrupole frequencies $\nu_Q[\text{Cr(A)}]$ and $\nu_Q[\text{Cr(B)}]$.

As was stated above, the quadrupole splitting of the NMR lines is not observed in ^{53}Cr NMR spectra in CrO_2 . It is possible that the quadrupole splitting is hidden in the spectrum width. As is known, if a homogeneous magnetic broadening

is less than the quadrupole splitting of the NMR line, the characteristic oscillations in the spin-echo decay should be observed, and the period of such oscillations is determined by the quadrupole frequency [20,35–37]. We have measured the spin-echo decay on both positions Cr(A) and Cr(B) at $T = 77$ K (Fig. 5) with the step of change of delay between two recording pulses equal to $1 \mu\text{s}$, but we have not observed any beats. This may be due either to the fact that homogeneous magnetic broadening is larger than the quadrupole splitting of the NMR line, or to the large inhomogeneity of distribution of quadrupole frequencies in the investigated material.

IV. CONCLUSION

We have performed ^{53}Cr NMR measurements on the high-purity polycrystalline sample to investigate the static and dynamic properties of a half-metallic ferromagnet CrO_2 . Two ^{53}Cr NMR lines, corresponding to magnetically nonequivalent chromium sites Cr(A) and Cr(B), were observed in the ferromagnetic phase of CrO_2 despite all the Cr ions being situated on the crystallographic equivalent sites. We measured the temperature dependences of the spin-lattice relaxation rate $(T_1)^{-1}$ for Cr(A) and Cr(B) nuclei in the ferromagnetic phase in the temperature range $T = 4.2\text{--}360$ K. While analyzing the temperature dependencies $(T_1)^{-1}$, it was stated that in the range of low temperatures ($T \leq 60$ K) the relaxation of nuclear magnetic moments is determined mainly by the temperature-proportional orbital contribution conditioned by the fluctuation of the orbital currents of d -band electrons.

It has been stated that at temperatures $T > 60$ K, the main mechanism leading to the nuclear spin-lattice relaxation is the so-called three-magnon scattering process, when the relaxation of the nuclear spin is accompanied by the absorption of a magnon and the creation of two magnons. This contribution is proportional to $T^{7/2}$. As for the two-magnon contribution to the spin-lattice relaxation of chromium nuclei, in the CrO_2 compound it is absent. Based on the analysis of the temperature dependences of $(T_1)^{-1}$ for Cr(A) and Cr(B) nuclei, we found that the valence state of chromium ions in these positions is the same and corresponds to valence Cr^{4+} , and the difference of resonance frequencies for Cr(A) and Cr(B) nuclei is conditioned by the different magnetic local fields in their location.

ACKNOWLEDGMENTS

The research was carried out within the state assignment of Ministry of Science and Higher Education of the Russian Federation (theme “Function” No. 122021000035-6).

- [1] K. Schwarz, CrO_2 predicted as a half-metallic ferromagnet, *J. Phys. F* **16**, L211 (1986).
- [2] S. P. Lewis, P. B. Allen, and T. Sasaki, Band structure and transport properties of CrO_2 , *Phys. Rev. B* **55**, 10253 (1997).
- [3] A. M. Korotin, V. I. Anisimov, D. I. Khomskii, and G. A. Sawatzky, CrO_2 : A Self-Doped Double Exchange Ferromagnet, *Phys. Rev. Lett.* **80**, 4305 (1998).

- [4] M. I. Katsnelson, V. Yu. Irkhin, L. Chioncel, A. I. Lichtenstein, and R. A. de Groot, Half-metallic ferromagnets: From band structure to many-body effects, *Rev. Mod. Phys.* **80**, 315 (2008).
- [5] R. J. Soulen Jr., J. M. Byers, M. S. Osofsky, B. Nadgorny, T. Ambrose, S. F. Cheng, P. R. Broussard, C. T. Tanaka, J. S. Moodera, A. Barry, and J. M. D. Coey, Measuring the spin

- polarization of a metal with a superconducting point contact, *Science* **282**, 85 (1998).
- [6] Y. Ji, G. J. Strijkers, F. Y. Yang, C. L. Chien, J. M. Byers, A. Anguelouch, G. Xiao, and A. Gupta, Determination of the Spin Polarization of Half-Metallic CrO₂ by Point Contact Andreev Reflection, *Phys. Rev. Lett.* **86**, 5585 (2001).
- [7] E. Z. Kurmaev, A. Moewes, S. M. Butorin, M. I. Katsnelson, L. D. Finkelstein, J. Nordgren, and P. M. Tedrow, Half-metallic electronic structure of CrO₂ in resonant scattering, *Phys. Rev. B* **67**, 155105 (2003).
- [8] P. Porta, M. Marezio, J. P. Remeika, and P. D. Dernier, Chromium dioxide: High pressure synthesis and bond lengths, *Mater. Res. Bull.* **7**, 157 (1972).
- [9] P. Schlottmann, Double-exchange mechanism for CrO₂, *Phys. Rev. B* **67**, 174419 (2003).
- [10] J. Dho, S. Ki, A. F. Gubkin, J. M. S. Park, and E. A. Sherstobitova, A neutron diffraction study of half-metallic ferromagnet CrO₂ nanorods, *Solid State Commun.* **150**, 86 (2010).
- [11] J. H. Shim, J. Dho, S. Lee, and D-H. Kim, Coexistence of Two Different Cr Ions by Self-Doping in Half-Metallic CrO₂ Nanorods, *Phys. Rev. Lett.* **99**, 057209 (2007).
- [12] S. Seong, E. Lee, H. W. Kim, B. I. Min, S. Lee, J. Dho, Y. Kim, J.-Y. Kim, and J.-S. Kang, Experimental evidence for mixed-valent Cr ions in half-metallic CrO₂: Temperature-dependent XMCD study, *J. Magn. Magn. Mater.* **452**, 447 (2018).
- [13] H. Takeda, Y. Shimizu, Y. Kobayashi, M. Itoh, T. Jin-no, M. Isobe, Y. Ueda, S. Yoshida, Y. Muraoka, and T. Yokoya, Local electronic state in the half-metallic ferromagnet CrO₂ investigated by site-selective ⁵³Cr NMR measurements, *Phys. Rev. B* **93**, 235129 (2016).
- [14] X. L. Wang, P. Z. Si, H. L. Ge, K. P. Shinde, K. C. Chung, and C. J. Choi, Synthesis, structure and magnetic properties of ultra-high purity CrO₂ prepared under high O₂-gas pressure, *Solid State Sci.* **67**, 72 (2017).
- [15] T. C. Farrar and E. D. Becker, *Pulse and Fourier Transform NMR: Introduction to Theory and Methods* (Academic, New York, 1971).
- [16] C. P. Slichter, *Principles of Magnetic Resonance* (Springer-Verlag, Berlin, 1989).
- [17] H. Nishihara, T. Tsuda, A. Hirai, and T. Shinjo, Nuclear magnetic resonance of Cr⁵³ in ferromagnetic, *J. Phys. Soc. Jpn.* **32**, 85 (1972).
- [18] E. A. Turov and M. P. Petrov, *Nuclear Magnetic Resonance in Ferro- and Antiferromagnets* (Holstead, New York, 1972).
- [19] V. V. Ogloblichev, Yu. V. Piskunov, and F. B. Mushenok, Magnetic order in the structurally disordered helicoidal magnet Cr_{1/3}NbS₂: NMR at ⁵³Cr nuclei, *J. Exp. Theor. Phys.* **125**, 317 (2017).
- [20] V. V. Ogloblichev, N. V. Baranov, P. A. Agzamova, A. Yu. Germov, N. M. Nosova, Yu. V. Piskunov, E. M. Sherokalova, N. V. Selezneva, A. F. Sadykov, and A. G. Smolnikov, Electronic states in ferromagnetic Cr_xNbSe₂ ($x = 0.33, 0.5$) studied by ⁵³Cr and ⁹³Nb NMR spectroscopy, *Phys. Rev. B* **104**, 245115 (2021).
- [21] A. G. Smol'nikov, V. V. Ogloblichev, S. V. Verkhovskii, K. N. Mikhalev, A. Yu. Yakubovskii, K. Kumagai, Y. Furukawa, A. F. Sadykov, Yu. V. Piskunov, A. P. Gerashchenko, S. N. Barilo, and S. V. Shiryayev, ⁵³Cr NMR study of CuCrO₂ multiferroic, *JETP Lett.* **102**, 674 (2015).
- [22] F. Bloch, Zur theorie des ferromagnetismus, *Z. Phys.* **61**, 206 (1930).
- [23] J. Korringa, Nuclear magnetic relaxation and resonance line shift in metals, *Physica* **16**, 601 (1950).
- [24] T. Moriya, Nuclear magnetic relaxation in ferromagnetic transition metals, *J. Phys. Soc. Jpn.* **19**, 681 (1964).
- [25] Y. Yafet and V. Jaccarino, Nuclear spin relaxation in transition metals; core polarization, *Phys. Rev.* **133**, A1630 (1964).
- [26] J. Winter, *Magnetic Resonance in Metals* (Clarendon Press, Oxford, 1971).
- [27] Y. Obata, Nuclear magnetic relaxation in transition metals, *J. Phys. Soc. Jpn.* **18**, 1020 (1963).
- [28] Y. Obata, Nuclear magnetic relaxation in transition metals. II. Relaxation due to quadrupole interaction, *J. Phys. Soc. Jpn.* **19**, 2348 (1964).
- [29] D. Beeman and P. Pincus, Nuclear spin-lattice relaxation in magnetic insulators, *Phys. Rev.* **166**, 359 (1968).
- [30] T. Moriya, Nuclear magnetic relaxation in antiferromagnetics, *Prog. Theor. Phys.* **16**, 23 (1956).
- [31] A. Narath, Nuclear magnetic resonance in magnetics and metals, in *Hyperfine Interactions* (Academic, New York, 1967).
- [32] V. Y. Irkhin and M. I. Katsnelson, Half-metallic ferromagnets, *Phys. Usp.* **37**, 659 (1994).
- [33] T. Oguchi and F. Keffer, Theory of the overhauser effect in ferro- and antiferromagnets, *J. Phys. Chem. Solids* **25**, 405 (1964).
- [34] I. V. Solovyev, I. V. Kashin, and V. V. Mazurenko, Mechanisms and origins of half-metallic ferromagnetism in CrO₂, *Phys. Rev. B* **92**, 144407 (2015).
- [35] H. Abe, H. Yasuoka, and A. Hirai, Spin echo modulation caused by the quadrupole interaction and multiple spin echoes, *J. Phys. Soc. Jpn.* **21**, 77 (1966).
- [36] H. Alloul and C. Froidevaux, Nuclear-magnetic-resonance spin echoes in alloys, *Phys. Rev.* **163**, 324 (1967).
- [37] V. V. Ogloblichev, A. G. Smolnikov, A. F. Sadykov, Y. V. Piskunov, A. P. Gerashenko, Y. Furukawa, K. Kumagai, A. Y. Yakubovsky, K. N. Mikhalev, S. N. Barilo, S. V. Shiryayev, and A. S. Belozherov, ¹⁷O NMR study of the triangular lattice antiferromagnet CuCrO₂, *J. Magn. Magn. Mater.* **458**, 1 (2018).